ce/papers Proceedings in civil engineering
Ernst & Sohn A Wiley Brand

ORIGINAL ARTICLE

eurosteel AMSTERDAM 2023 Ernst & Sohn A Wiley Brand

Experimental Investigation of Sheathed Cold-Formed Steel Sigma Studs Under Compression Loading

Amir M. Yousefi[1] | Bijan Samali[1] | Yang Yu[2]

Correspondence

Dr. Amir M. Yousefi
School of Engineering, Design and Built Environment
Western Sydney University
Kingswood NSW 2747
Australia
Email: amir.yousefi@western-sydney.edu.au

[1] Western Sydney University, Sydney, Australia
[2] University of New South Wales, Sydney, Australia

Abstract

Cold-formed steel sections are used to form various components of low-and medium-rise buildings. Such sections are commonly constructed with sheathing board, providing thermal and acoustic separation between interior partitions. In contemporary projects, these sheathing boards have been used to provide bracing and increasing lateral stiffness. The strength and stiffness of sheathing-braced structural assemblies is governed by connections between framing elements and sheathing components. This paper describes an experimental investigation of stability and strength of sheathed cold-formed steel lipped sigma wall studs under compression loading. A total of 35 experimental tests conducted covering various parameters including, sheathing plasterboard thickness, stud and track thickness, plasterboard configuration and density. Sheathing density and thickness are found to be significant in impacting the compression strength of the sheathed cold-formed steel lipped sigma studs. A clear pattern was noted between plasterboard material and thickness on the stability and strength of the sheathed stud. It is found that higher density boards provided the greatest restraint against buckling, as did increased thicknesses. Isolating direct loading of the sheathing, and Composite action between the stud and sheathing are shown to be significant in determining the strength and controlling limit state of the stud.

Keywords

Cold-formed steel, Experimental investigation, Compression loading, Sigma stud.

1 Introduction

Cold-formed steel (CFS) sections have been used in construction since the mid-19th century in the United States and Great Britain, with widespread adoption starting after the introduction of design standards and codes in 1946. Low material costs, high strength-to-weight ratios, simple installation, and good durability make cold-formed steel sections an attractive alternative to heavier hot-rolled steel and less durable timber components in low- to mid-rise construction [1]. CFS wall frames are typically assembled from a combination of vertical CFS studs mounted to horizontal tracks (see Fig. 1). Sheathing boards, primarily consisting of wood, cement or gypsum are fastened to either one or both sides of the track/stud assembly, forming a wall panel (see Fig. 2). In addition to providing fire and acoustic buffering, these wall panels have been used to resist both lateral and vertical loads [1].

While recent research focused on the behaviour of CFS structural beams [2-6], limited studies are available on structural behaviour of sheathed CFS studs under compression. In the literature, Peck et al. [7] assessed the in-plane response of CFS- gypsum shear walls. As part of the investigation, the effect of loading patterns on connection behaviour was assessed. Comparing the load-displacement curves of identical specimens under monotonic and cyclic loading revealed minimal change in initial response. Against expectations, the peak strength values of the cyclic tests were higher than their monotonic counterparts. Based on these observations, the author proposed that monotonic tests may be suitable for seismic and wind load assessments without accounting for the effect of cyclic loads. This conclusion conflicts with a similar study by Wu et al. [8], that suggests cyclic load patterns result in lower ultimate load capacities due to accumulated screw-sheathing interface damage, indicating the need for a reduction factor to apply to structures designed using monotonic test values alone.

An experimental investigation by Landolfo Corte and Fiorino [9] compared the behaviour of CFS-sheathing wall panels lined with oriented strand boards (OSB) or gypsum wallboards (GWB). The test program included 32 small-scale specimens, with variable parameters including sheathing material, loading direction (perpendicular or parallel to the OSB strand), screw to loaded edge distance, load method (monotonic compression, tension or cyclic)

https://doi.org/10.1002/cepa.2492
wileyonlinelibrary.com/journal/cepa

and loading rate. The sheathing material had a significant effect on connection behaviour, with OSB sheathings exhibiting greater strength and energy absorption than identical GWB specimens, however GWB specimens exhibited greater stiffness. As expected, increased fastener-edge distances saw an increase in ultimate connection capacity and stiffness. Changes to monotonic loading rates had minimal observable impact on connection capacities

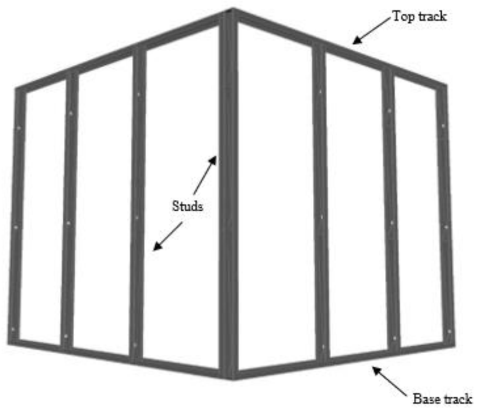

Figure 1 Tracks and studs in a basic wall frame

Nithyadharan and Kalyanaraman [10] proposed an updated testing method to better represent the behaviour of screw connections in CFS wall panels under lateral loads. Most experimental studies using small-scale specimens apply loads perpendicular to the free edge of the sheathing. The authors argued that this configuration does not provide a realistic simulation of connection and component stresses in actual structures. The assembly employed in this study applied axial loads to a CFS stud running parallel to the free sheathing edge, connected to two sheathing panels to a second, restrained CFS stud. In addition to assessing the suitability of this new configuration, the effect of sheathing thickness and screw edge distance on connection behaviour under monotonic and cyclic loads was assessed. Behaving consistently with traditional configurations, the peak strength and stiffness of the screw connections increased with board thickness and edge distance. Additionally, ductility was greatly reduced with a reduction in edge distance, however remained relatively constant despite reducing board thickness. Aspects of this experimental setup are used in the proposed study, particularly the parallel orientation of the applied load and screw fasteners.

An extensive study on the effect of stud thickness, plasterboard sheathing thickness, screw end distance, sheathing orientation, fastener diameter and fastener spacing on the in-plane strength and stiffness of CFS-to-sheathing was conducted by Abeysiriwardena and Mahendran [11]. Failure modes were typically a combination of screw tilting, screw pull-through and plasterboard bearing failure. Due to the non-uniform nature of the plasterboard material, some variation load-displacement behaviour variation was observed between identical specimens. Three plasterboard thicknesses were assessed, from 10 mm to 16 mm. It was noted that the reduced porosity of the 16 mm samples was responsible brought less load-displacement behaviour variations compared to thinner sheets. To ensure this porosity induced variation did not contaminate the output data, tests were repeated on four identical specimens, and their recorded load-displacement curves averaged. Given the nature of the experimental setup, with equal load distribution between all four screw fasteners per sheathing board, the total stiffness of the test assembly could be converted to the equivalent stiffness of a single connection. This approach mitigated inaccuracies due to unexpected variables, such as screw over-driving and localised plasterboard defects. Comparing the load-displacement responses of varied test configurations, the effect of the previously listed design parameters was assessed. As expected, specimens with the thinnest sheathing layers exhibited pure bearing failure only, with no screw tiling or pull-through observed. Discussed later in this paper, the authors conducted a numerical study, validating their model with data from these tests.

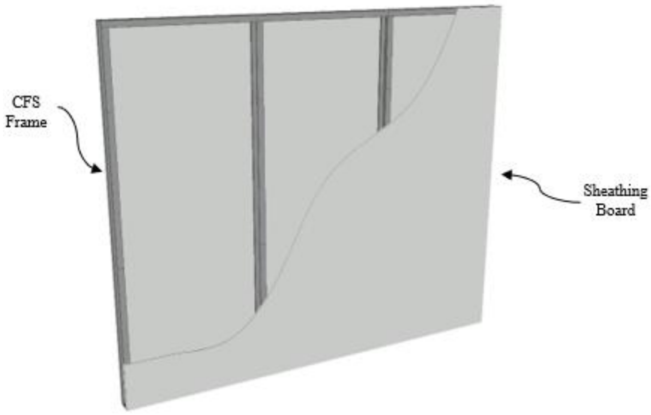

Figure 2 Cut-away of sheathed CFS wall frame

Wu and Sang [12] investigated a novel stud-to-sheathing connection reinforcement method using both small- and full-scale specimens under monotonic and cyclic loads. Installing CFS strips between the screw fastener head and the sheathing material, shear capacity of reinforced samples was up to 1.53 times higher than unreinforced specimens. The limiting failure modes observed in the small-scale tests included screw tilting, sheathing pull-through, sheathing bearing failure and screw fracture. Without additional CFS strip reinforcement, combined tilting and pull-through failure was encountered. The resistance against tilting provided by the reinforcement strip delayed tilting and subsequent fastener pull-through, leading to screw fracture instead. Increasing sheathing thickness saw a corresponding increase in connection peak strength and stiffness. Additionally, OSB panels produced higher peak strength and elastic stiffness values compared to identical gypsum panels. This study provided a valuable insight into the factors leading to fastener tilting failure modes, and a similar experimental study is proposed later in this paper.

Vieira and Schafer [13] conducted an experimental investigation into the stability and strength of axially compressed studs, both with and without sheathing boards of varying material attached to the stud flanges. 26 tests were conducted, with variables including sheathing configurations, axially loaded stud length and end boundary conditions. The experimental assemblies developed for the 2011 study are geometrically similar those employed in the perpendicular tests. Similarly, the LVDT placement and subsequent result processing will be mirrored in the buckling assessment component of this study. All specimens sheathed on two sides received adequate restraint to restrict global and distortional buckling, demonstrating the contribution of sheathing boards to the compressive capacity of CFS studs. With both global and distortional buckling restricted, local buckling became the controlling limit state in all sheathed samples. However, none of the aforementioned studies conducted a experimental tests on sheathed cold-formed steel sigma stud with different thickness of plasterboards under compression, and no test results were reported. This issue is addressed herein. A total of 35 experimental tests conducted in this paper covering various parameters including, sheathing plasterboard thickness, stud and track thickness, plasterboard configuration and density. Sheathing density and thickness are found to be significant in impacting the compression strength of the sheathed cold-formed steel lipped sigma studs. A clear pattern was noted between plasterboard material and thickness on the stability and strength of the sheathed stud. It is found that high-er density boards provided the greatest restraint against buckling, as did in-creased thicknesses. Finally the effect of stud thickness on compression capacity of the sheathed studs is described.

2 Experimental Investigation

2.1 Specimen nomenclature

Specimen nomenclature is considered to simply determine and identify the specimens in the experimental programme. Rather than identifying the number of fasteners per loaded edge, the number of screws per compressed stud flange is noted. The compression specimen code structure is shown in Figure 3 and specimen parameters listed in Table 1. Figure 4 shows stud sections used in the experimental programme.

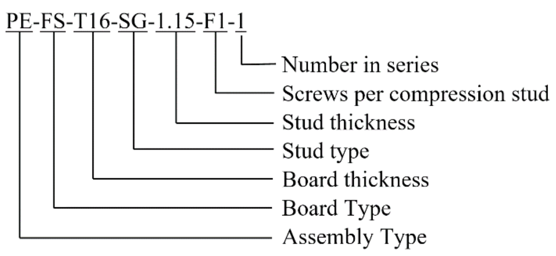

Figure 3 Compression specimen nomenclature

2.2 Specimen assembly

The compression specimen assemblies consist of two gypsum sheathing boards fastened to two horizontal CFS studs. Compression assemblies are characterized by a third CFS stud, mounted vertically between the two horizontal sections. The screw fasteners joining the horizontal and vertical studs do not pass through the sheathing material. This ensures the compressive load is primarily transmitted through the vertical stud, not the sheathing board. Two to four additional screw fasteners connect the sheathing board to the vertical CFS stud (see Fig. 5).

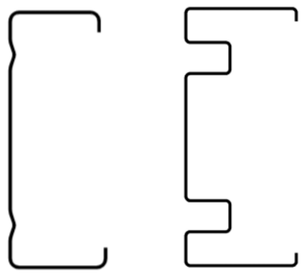

Figure 4 Stud sections in the experimental programme

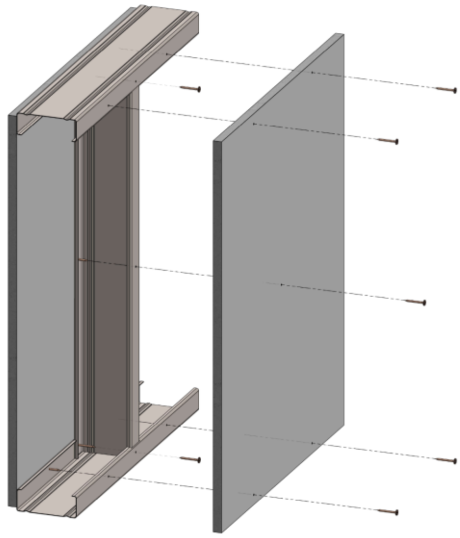

Figure 5 Test specimen assembly sequence

2.3 Instrumentation

As shown in Fig. 6, Four linear potentiometers were used to record vertical and horizontal displacements. Two linear potentiometers were mounted to record vertical displacements of the top stud as loads were applied. These vertically oriented LPs were mounted with the probes contacting the centreline of the upper stud, approximately 1.5 cm from the outside edge. While vertical displacement along the centreline of the upper stud was expected to remain constant, both outside ends exhibited significant deformation relative to the stud midpoint. Given the severity of this displacement in some cases, the crosshead displacement recorded by the Instron UTM is used to represent average vertical displacement. The remaining two LPs were mounted to measure in-plane and out-of-plane deflections at the mid-point of the stud under compression.

2.4 Test set-up

Significant deformation of the bolted SHS load assembly was noted during a proof-of-concept trial of the compression assembly testing method. Previous studies using similar experimental assemblies [13] encountered peak loads greater than 50 kN. Loads greater than 30 kN resulted in noticeable deformation of the original SHS load assembly. This deformation would reduce the accuracy of the load-displacement curves, so an alternative load-distribution method was developed. Compressive loads were transmitted along the entire length of the top stud through a solid high-strength steel plate, shown in Figure 7. A smaller spacer plate was also used to ensure loads were applied across the entire jaw assembly, minimizing the risk of damage to the Instron apparatus. Unlike the shear specimen load assembly, this assembly does not entirely resist lateral forces or moments. Given the symmetrical nature of the assemblies, eccentric loads due to these moments and lateral forces were negligible.

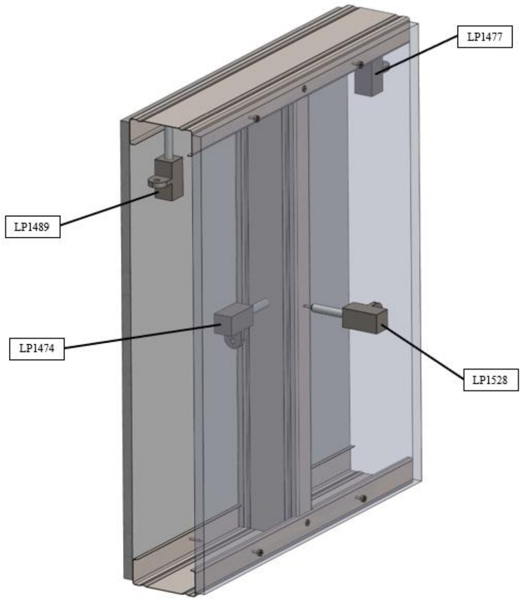

Figure 6 Test specimen assembly

Figure 7 Experimental test set-up

3 Experimental results

The primary objective of the practical experiments was to demonstrate the effect of varying assembly parameters on the strength and stiffness of CFS-gypsum connections. A qualitative assessment of observed failure modes was recorded throughout each test, and quantitative data was recorded to develop a load-displacement relationship for each specimen. Combining these separate datasets revealed key trends as specimen properties were varied. Table 1 and 2 show the specimen details and test results, respectively.

Table 1 Specimen details in the experimental programme

Board Thickness	Stud Type	Stud Thickness	Screws per stud	Short Code
mm		*mm*		
T16	SG	1.15	1	PE-FS-T16-SG-1.15-1
T16	SG	1.15	1	PE-FS-T16-SG-1.15-2
T16	SG	1.15	1	PE-FS-T16-SG-1.15-3
T13	SG	1.15	1	PE-FS-T13-SG-1.15-1
T13	SG	1.15	1	PE-FS-T13-SG-1.15-2
T13	SG	1.15	1	PE-FS-T13-SG-1.15-3
T16	SG	1.15	2	PE-FS-T16-SG-1.15-1
T16	SG	1.15	2	PE-FS-T16-SG-1.15-2
T16	SG	1.15	2	PE-FS-T16-SG-1.15-3
T13	SG	1.15	2	PE-FS-T13-SG-1.15-1
T13	SG	1.15	2	PE-FS-T13-SG-1.15-2
T13	SG	1.15	2	PE-FS-T13-SG-1.15-3
T13	AC	0.55	1	PE-FS-T13-AC-0.55-1
T13	AC	0.55	2	PE-FS-T13-AC-0.55-1
T16	AC	0.55	1	PE-FS-T16-AC-0.55-1
T16	AC	0.55	2	PE-FS-T16-AC-0.55-1

Increased plasterboard thicknesses resulted in an increase in peak compressive strength of the assembly. Shown in Figure 84, a 18.75% increase in fire rated plasterboard thickness (13 mm to 16 mm) resulted in an average 10% increase in peak strength. As shown in Figure 8 the first, second, and third phase stiffnesses remained relatively consistent between 13 mm and 16 mm thick specimens. Sound rated specimens exhibited a similar trend, with a 23% increase in plasterboard thickness resulting in an 8% increase in peak strength, shown in Figure 8.

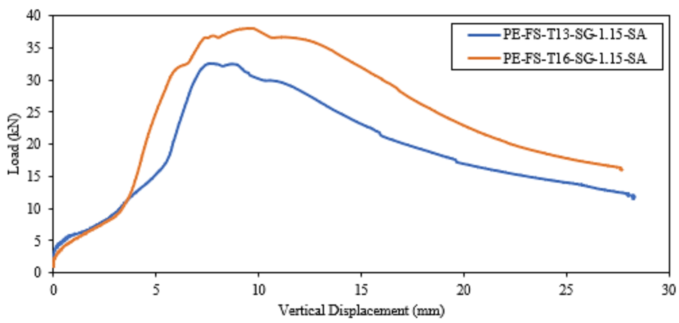

Figure 8 FS-SA Load-Vertical Displacement Comparison

4 Failure modes

Failure mode progression was largely consistent across all specimens. As shown in Figure 10, the load-vertical displacement curve is separated into three distinct phases. The first phase starts at the initial application of the compressive load to the assembly. Through this phase, minor screw tilting and pull-through was observed in the top fasteners. Additionally, negligible in-plane and out-of-plane deflection of the vertical stud is observed. This phase continues until the upper track web displaced enough to contact the top of the compressive stud.

Table 2 Compression Test Peak Loads and Buckling Modes

Specimen Code	P_{peak} kN	Buckling Mode
PE-FS-T16-SG-1.15-SA-1	38.02	$Local_{top}$
PE-FS-T16-SG-1.15-SA-2	37.13	$Local_{top}$
PE-FS-T16-SG-1.15-SA-3	38.93	$Local_{top}$
PE-FS-T13-SG-1.15-SA-1	32.45	$Local_{top}$
PE-FS-T13-SG-1.15-SA-2	35.32	$Local_{base}$
PE-FS-T13-SG-1.15-SA-3	34.18	$Local_{top}$
PE-FS-T16-SG-1.15-SB-1	35.98	$Local_{base}$
PE-FS-T16-SG-1.15-SB-3	38.49	$Local_{top}$
PE-FS-T13-SG-1.15-SB-1	34.88	$Local_{top}$
PE-FS-T13-SG-1.15-SB-2	35.97	$Local_{top}$
PE-FS-T13-SG-1.15-SB-3	40.16	$Local_{base}$
PE-FS-T13-AC-0.55-SA-1	28.87	$Global$
PE-FS-T13-AC-0.55-SB-1	30.63	$Global$

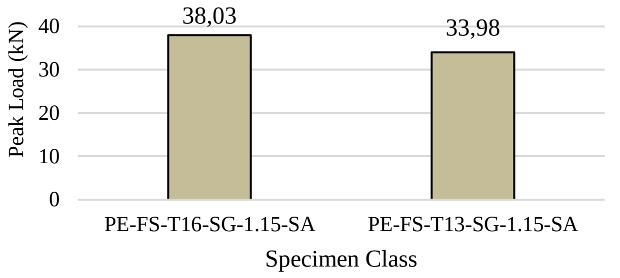

Figure 9 Peak Load Comparison

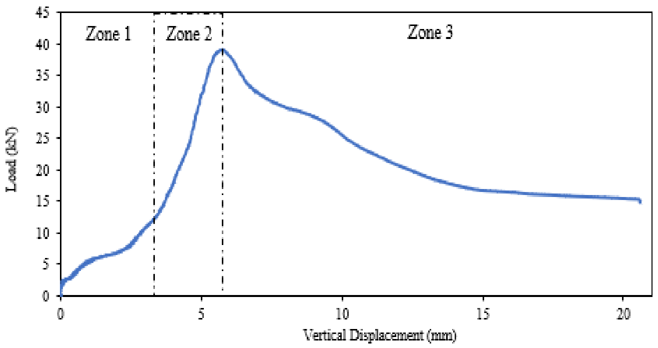

Figure 10 Vertical Load-Displacement Curve (PE-FS-SG-T13-1.15-SA)

The second phase continues from the initial stud-track contact until the peak load is reached. During this phase, the vertical stud is engaged in direct bearing against the upper and lower track webs. The vertical load-displacement gradient increases significantly, given the CFS stud's axial stiffness is greater than the plasterboard under compression. During this phase, the in-plane deflection of the vertical stud typically increased linearly as the vertical stud buckled. The 'post-peak' phase continues from the buckling point until the end of the end of the test. In most cases, deformation of the top stud-track interface forced the sheathing boards out post-peak.

Failure modes started with minor screw tilting, pull-through and edge cracking was observed, with damage progression varying slightly between plasterboard type and thickness. Buckling is defined as a "limit state of sudden change in the geometry of a structure or any of its elements under a critical loading condition". (Yu et al. [14]) Two distinct buckling modes were observed through these compression tests, classified as local buckling and global buckling. Local buckling is characterised by the deformation of one or more individual plates of a loaded section. Figure 11 shows local buckling failure, while Figure 12 shows global buckling of the deformed studs.

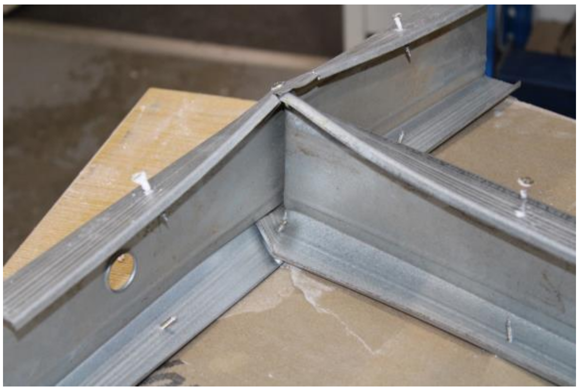

Figure 11 Local Buckling Failure (PE-SS-T10-SG-1.15-SA-2)

Figure 22 Global Buckling (PE-FS-T13-AC-0.55-SB-1)

5 Effect of stud thickness

Stud thickness was varied using 1.15 mm Sigma sections and 0.55 mm Acoustic sections. As expected, 1.15 mm specimens exhibited higher peak loads, as shown in Figure 87. This trend matched expected behaviour, as thicker sections are less susceptible to global buckling. Additionally, a significant increase in post-buckling stiffness was noted in 1.15 mm specimens, resulting in a longer third phase, shown in Figure 14. Curiously, increased stud thickness does not appear to significantly impact assembly stiffness prior to buckling. It should be noted that these variances in assembly stiffness and peak strength are not attributed soley to the ply thickness of the compressed stud. Since 0.55 mm thicknesses were only available as part of the acoustic stud product line, the loaded cross section varies between 0.55 mm and 1.15 mm specimen

Figure 13 Vertical and lateral in-plane LP placement (post-test)

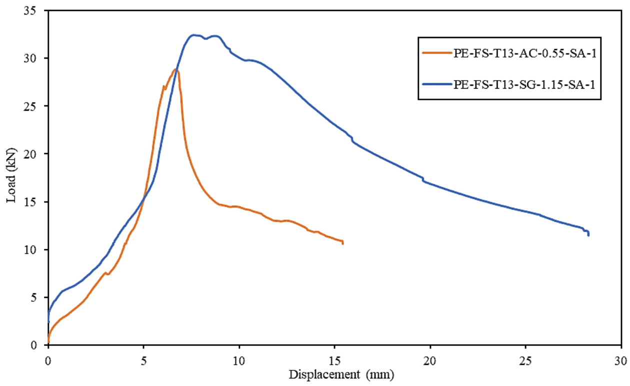

Figure 14 Stud Thickness Assembly Stiffness Comparison

6 Conclusions

This paper has discussed an experimental study investigating the behaviour of cold-formed steel to plasterboard connections under shear load, and the behaviour of plasterboard sheathed cold-formed steel elements under compression. Key assembly parameters, including plasterboard material, plasterboard thickness, stud thickness and stud section were varied, and their impact on peak loads and connection stiffnesses assessed. A series of 35 specimens were tested, demonstrating the contribution of sheathing boards to the compressive strength of an axially loaded stud. These tests also assessed the effect of stud thickness on compression capacity of studs. A clear pattern was noted between plasterboard material and thickness on the stability and strength of the sheathed stud. It was found, higher density boards provided the greatest restraint against buckling, as did increased thicknesses. Several areas were noted for future research as part of this study. The effect of reinforcement orientation through sheathing plasterboards was not assessed and may influence the strength and stiffness of connections under shear loading.

References

[1] Vieira, L & Schafer, B 2012, "Lateral stiffness and strength of sheathing braced cold-formed steel stud walls", Engineering Structures, vol. 37, pp. 205-213.

[2] Rezvani, F.H.; Yousefi, A.M.; Ronagh, H.R. Effect of span length on progressive collapse behaviour of steel moment resisting frames. Structures. 2015, 3, 81-89.

[3] Yousefi, A.M.; Lim, J.B.P.; Clifton, G.C. Web crippling behaviour of unlipped cold-formed ferritic stainless steel channels subject to one-flange loading. J. Struct. Eng. 2018, 144, 04018105.

[4]Yousefi, A.M.; Samali, B.; Hajirasouliha, I. Experimental and numerical investigations of cold-formed austenitic stainless steel unlipped channels under bearing loads. Thin-Wall. Struct. 2020, 152, 106768.

[5] Yousefi, A.M.; Samali, B. Design of cold-formed ferritic stainless steel unlipped channels with offset web openings and unfastened flanges subject to web bearing failure under one-flange load scenarios. Structures. 2020, 27, 194-211.

[6] Mohammadjani, C.; Yousefi, A.M.; Cai, S.Q.; Clifton, G.C.; Lim, J.B.P. Strength and stiffness of cold-formed steel portal frame joints using quasi-static finite element analysis. Steel Compos. Struct., Int. J. 2017, 25, 727-734.

[7] Peck, Q., Rogers, N. and Serrette, R., 2012. Cold-Formed Steel Framed Gypsum Shear Walls: In-Plane Response. Journal of Structural Engineering, 138(7), pp.932-941.

[8] Wu, H., Chao, S., Li, Y. and Sang, L., 2020. Experimental investigation of strengthened screw connection and application in CFS shear walls. Journal of Constructional Steel Research, 168.

[9] Landolfo, R., Della Corte, G. and Fiorino, L., 2006. Shear Behavior of Connections between Cold-Formed Steel Profiles and Wood or Gypsum-Based Panels: An Experimental Investigation. Structures Congress 2006.

[10] Nithyadharan, M. and Kalyanaraman, V., 2011. Experimental study of screw connections in CFS-calcium silicate board wall panels. Thin-Walled Structures, 49(6), pp.724-731.

[11] Abeysiriwardena, T., Peiris, M. and Mahendran, M., 2021. Local in-plane strength and stiffness of stud-to-sheathing fastener connections in LSF wall panels. Thin-Walled Structures, 160, p.107383.

[12] Wu, H., Chao, S., Li, Y. and Sang, L., 2020. Experimental investigation of strengthened screw connection and application in CFS shear walls. Journal of Constructional Steel Research, 168.

[13] Vieira, L., Shifferaw, Y. and Schafer, B., 2011. Experiments on sheathed cold-formed steel studs in compression. Journal of Constructional Steel Research, 67(10), pp.1554-1566.

[14] Yu, W, LaBoube, R & Chen, H 2019, Cold-formed steel design, 5th edn, John Wiley & Sons.

[15] Yousefi, A.M.; Samali, B.; Yu, Y. Shear Behaviour and design of cold-formed ferritic stainless steel channels

with circular web openings. Structures. 2021, 33, 4162-4175.

[16] Yousefi, A.M.; Samali, B.; Yu, Y. Unified design equations for web crippling failure of cold-formed ferritic stainless steel unlipped channel-sections with web holes. Journal of Building Engineering. 2022, 45, 103685.

[17] Yousefi, A.M.; Lim, J.B.P.; Clifton, G.C. Cold-formed ferritic stainless steel unlipped channels with web perforations subject to web crippling under one-flange loadings. Construct. and Build. Mats. 2018, 191, 713-725.

[18] Yousefi, A.M.; Lim, J.B.P.; Clifton, G.C. Web crippling strength of perforated cold-formed ferritic stainless steel unlipped channels with restrained flanges under one-flange loadings. Thin-Wall. Struct. 2019, 137, 94-105.